

EXPERIMENTAL EVIDENCE FOR ELECTRON VELOCITIES AS
THE CAUSE OF COMPTON LINE BREADTH WITH THE
MULTICRYSTAL SPECTROGRAPH

BY JESSE W. M. DUMOND AND HARRY A. KIRKPATRICK
CALIFORNIA INSTITUTE OF TECHNOLOGY, PASADENA

(Received December 1, 1930)

ABSTRACT

The main purpose of this research was to test the correctness of the assumption that the initial velocities of electrons in the scattering body cause the observed breadth of the Compton shifted line. The test consists in observing the natural breadths of the Compton line for different scattering angles and primary wave-lengths and comparing these with the functional dependence of breadth on scattering angle and primary wave-length deduced theoretically on the basis of the assumption under test. It is shown in this paper that if electron velocities are the cause of the breadth then this breadth should increase with the scattering angle according to the approximate formula $\Delta\lambda = K\cos\frac{1}{2}\theta$ where $\Delta\lambda$ is the breadth, θ the scattering angle and K a constant depending on the primary wave-length and the scattering substance. For the same scattering angle and substance the breadth should be proportional to the primary wave-length.

The experimental test was made with the multicrystal spectrograph of fifty units herein briefly described. Three scattering angles were used, $63\frac{1}{2}^\circ$, 90° , 156° , the inhomogeneity in each case being less than one degree. The spurious breadth due to this inhomogeneity is negligible compared to the observed breadths. Three very clear cut spectrograms are reproduced representing MoK radiation scattered from graphite together with microphotometer curves taken from them. The increase of shifted line breadth with scattering angle is clearly visible and compares favorably with the theoretical prediction. The increase of line breadth with increasing primary wave-length comparing the breadths of shifted α_1 and shifted β_1 lines seems just detectable. The unshifted lines are very sharp, the α doublet being clearly resolved. Incidentally the cause of the heavy background so frequently observed on Compton effect spectrograms has been found to be non-selective scattering at the crystals and a great reduction of background and improvement in contrast has been effected by the use of baffles to diminish this effect.

The observed shift of the Compton line supports Compton's formula $\delta\lambda = (h/mc)(1 - \cos\theta)$ where $h/mc = 24.2X.U.$

The shifted line breadths are greater than those reported by Gingrich and Barden and possibly Ross but seem to be in general accord with previous breadths obtained at this laboratory and with those of H. M. Sharp and of F. L. Nutting. The reason for these discrepancies is unknown. The possibility of double or higher multiplicities of scattering is being investigated. (See note added in proof at the end of this article.)

PURPOSE OF THE INVESTIGATION

NEARLY all investigators have observed that the Compton shifted line is broader than either the unshifted line or the primary line. Jauncey,¹ Wentzel² and DuMond³ have each attributed the observed breadth of the

¹ Jauncey, Phys. Rev. **25**, 314-322 (1925); 723-736 (1925).

² Wentzel, Zeits. f. Physik **43**, 188 (1927); **43**, 779-787 (1927).

³ DuMond, Phys. Rev. **33**, 643-658 (1929).

Compton line to the velocities possessed initially by the electrons in the scattering body. DuMond³, and almost simultaneously, Chandrasekhar⁴ have applied the above assumption to the conduction electrons in the interatomic spaces of the crystal lattice in the case of electrically conducting scatterers and the former has shown that the results compared with his observed Compton line structures seem to support favorably the new Fermi, Pauli, Dirac, Sommerfeld statistics for such conduction electrons. It is important to test the correctness of the assumption that the velocities (or more accurately the momenta) of electrons bound in atoms or in the interatomic spaces of the crystal lattice are responsible for Compton line broadening.

We have attempted to test this assumption by observing the dependence of Compton line breadths on the scattering angle in the case of MoK radiation scattered by graphite and comparing this with the theoretical functional dependence to be expected if the assumption be correct that electron velocities cause the breadth. The theoretical considerations will be dealt with first.

PART I. THEORETICAL

GENERAL NON-MATHEMATICAL DISCUSSION

Before passing to the analytical argument we venture to offer a verbal discussion of the cause of Compton line-breadth regarded as a Doppler effect of the random-moving electrons scattering the radiations in order to serve as a guide to the reader through the cold formality of the analysis. The use of the words "Doppler effect" we insist shall not be naïvely interpreted as committing us to any *mechanism* (classical, undulatory or otherwise) to "explain" the wave-length modification associated with scattering of radiation by a moving scattering agent. It is now an old story that the Doppler effect from a moving scatterer can be equally well derived on either the extreme undulatory hypothesis or the extreme corpuscular hypothesis—the latter derivation requiring only the quantum application of the laws of conservation of momentum and energy to the elementary scattering process. *Furthermore the interpretation of the broadening of the Compton line as a Doppler effect of the motion of weakly bound electrons here presented is a perfectly valid first approximation to the quantum mechanical treatment of the effect as given by Wentzel, Gordon and others.* The condition for such validity is that the binding energy of the electron shall be small compared to the energy imparted to the electron in the scattering process. This condition is fulfilled in the present case.

When x-radiation is scattered by the electrons in a scattering body the total effect of the motion of the electrons may be thought of as a superposition of two "Doppler effects"—one caused by the initial motion of the electrons, the other caused by the motion imparted to the electrons by the radiation in the scattering process. The first Doppler effect can in the case of random electron motions have either a positive or a negative sign, depending on whether the electron's initial velocity before scattering has a component directed toward or away from the vector expressing the change in momentum suffered by the

⁴ Chandrasekhar, Royal Soc. Proc. **A125**, 231–237 (1929).

radiation in the scattering process. The second Doppler effect can have only one sign (corresponding to an increase in scattered wave-length over incident wave-length) because the momentum imparted to the electron in the scattering process must always be opposite in direction to the vector change in momentum of the radiation. Both Doppler shifts will vanish for zero scattering angle and be a maximum for a scattering angle of 180° .

The first Doppler shift having either positive or negative sign accounts for the broadening of the Compton modified line. The second Doppler shift accounts for the justly famous shift of the Compton line toward longer wave-lengths.

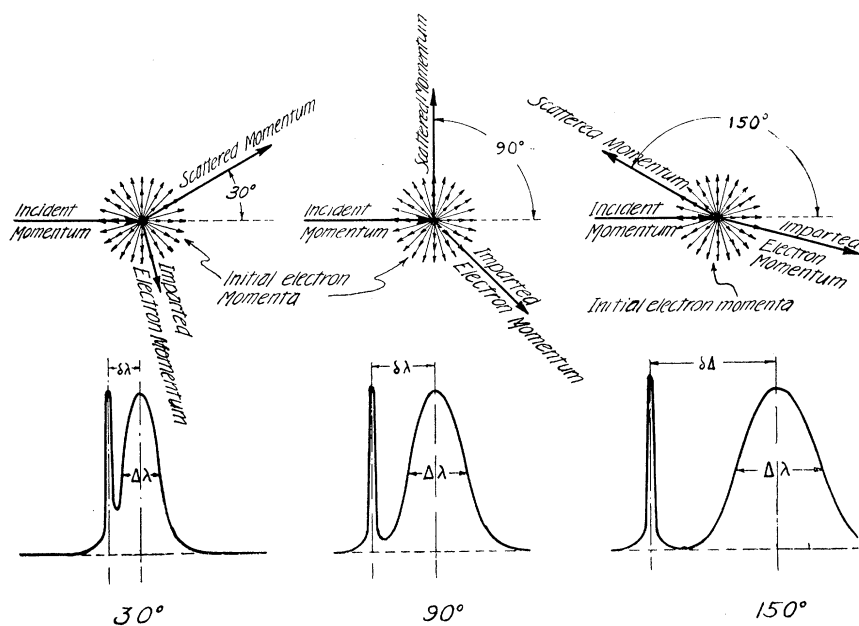


Fig. 1. Schematic illustration of Compton scattering by randomly directed moving electrons for three scattering angles together with idealized spectra of the resulting scattered radiation for each case. The constancy of the initial momentum and the increase in the momentum imparted to the electron with increasing scattering angle is shown. In this diagram the randomly directed initial momenta are *much exaggerated* relative to the imparted momentum.

Let us define the relative breadth $\Delta\lambda_r$ as the breadth at any scattering angle divided by the breadth at 180° scattering angle (maximum breadth). Let us also define the relative shift $\delta\lambda_r$ in an entirely analogous way. The relative breadth and the relative shift will be shown to be given by⁵

⁵ It is interesting to note that the relative shift is the *square* of the relative breadth. This is because the *shift* increases with the scattering angle due to *two* causes, (1st because the Doppler effect from *any* moving scatterer increases with the scattering angle, 2nd because the velocity of the moving scatterer itself increases with the scattering angle in the case of the Compton shift) while the *breadth* increases with the scattering angle due to only the first of these causes alone, the velocity of the scattering electron accountable for the breadth being independent of the scattering angle.

$$\text{Breadth } \Delta\lambda_r = \sin \frac{1}{2}\theta \text{ approximately}$$

$$\text{Shift } \delta\lambda_r = \sin^2 \frac{1}{2}\theta$$

Fig. 1 shows diagrammatically the vectors of light momentum, random initial electron momentum and momentum imparted by the scattering process to the electron for three scattering angles together with an idealized Compton shifted line spectrum for each case. In Fig. 2 the relative breadth and relative

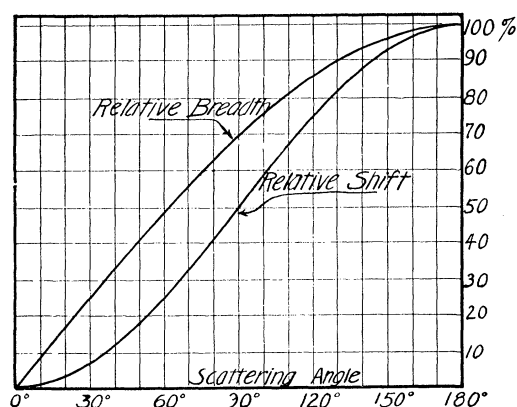


Fig. 2. Relative breadth and relative shift computed for molybdenum *K* radiation using Eqs. (10) and (8). The relative breadth is the quotient of the breadth at any scattering angle by the maximum breadth which occurs at 180°. The relative shift is similarly defined.

shift are plotted as functions of the scattering angle. In this case the more accurate formula derived below has been used for the computations of relative breadth.

ANALYTICAL SOLUTION

Case of one free scattering electron only. The solution of this case in the form of Eq. (5) was obtained by de Broglie in his "Ondes et Mouvements Fascicule" 1. pp. 94-95. The primary radiation is taken as travelling in the positive *x*-direction. θ is the angle of scattering; ν_1 is the initial frequency; $\beta_1 c$ the speed of the electron before scattering, a_1, b_1, c_1 , the direction cosines of its velocity and $a_1 = \cos \theta_1$ so that θ_1 is the angle between the initial electron momentum and the initial light momentum. ν_2 is the frequency of the scattered quantum and its direction of propagation has the direction cosines p, q, r , making angle ϕ with the initial velocity of the electron and angle θ with *OX*. Fig. 3 shows the relations of the various vectors and angles. Evidently

$$\cos \phi = a_1 p + b_1 q + c_1 r$$

$$p = \cos \theta.$$

The recoiling electron has a final speed $\beta_2 c$ in the direction defined by the cosines a_2, b_2, c_2 .

The following four equations express the conservation of energy and of the

three rectangular components of momentum before and after the scattering process.

$$h\nu_1 + m_0c^2/(1 - \beta_1^2)^{1/2} = h\nu_2 + m_0c^2/(1 - \beta_2^2)^{1/2} \quad (1)$$

$$h\nu_1/c + (m_0\beta_1c/(1 - \beta_1^2)^{1/2})a_1 = (h\nu_2/c)p + (m_0\beta_2c/(1 - \beta_2^2)^{1/2})a_2 \quad (2)$$

$$(m_0\beta_1c/(1 - \beta_1^2)^{1/2})b_1 = (h\nu_2/c)q + (m_0\beta_2c/(1 - \beta_2^2)^{1/2})b_2 \quad (3)$$

$$(m_0\beta_1c/(1 - \beta_1^2)^{1/2})c_1 = (h\nu_2/c)r + (m_0\beta_2c/(1 - \beta_2^2)^{1/2})c_2 \quad (4)$$

Eliminating a_2 , b_2 , c_2 and β_2 and letting $\alpha = h\nu_1/m_0c^2$ we obtain on solving for the change in wave-length,

$$\lambda_2 - \lambda_1 = \frac{\beta_1(\cos \theta_1 - \cos \phi)}{1 - \beta_1 \cos \theta_1} \lambda_1 + \frac{2\alpha\lambda_1 \sin^2 \frac{1}{2}\theta}{1 - \beta_1 \cos \theta_1} \quad (5)$$

where the second term accounts for the simple Compton shift and the first term represents the modification caused by the electron's initial speed β_1 .

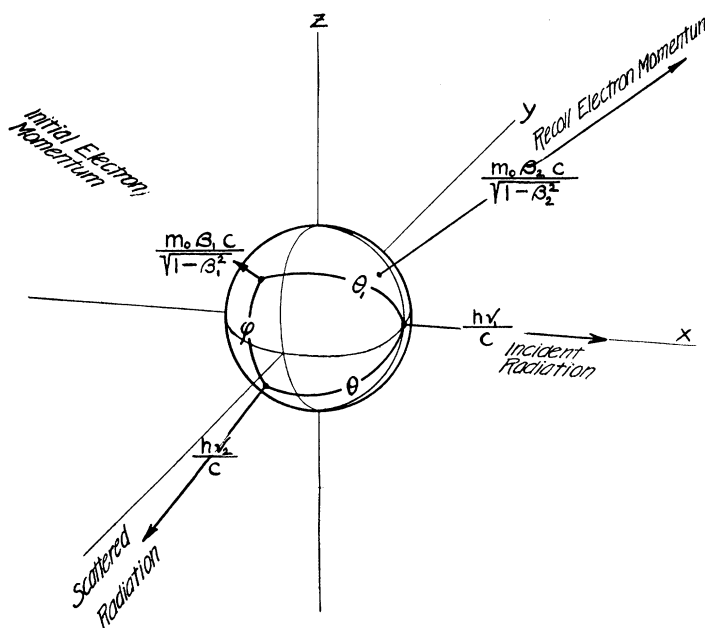


Fig. 3. Illustrating the various angles and vectors involved in Compton scattering by an electron possessing initial momentum. The initial electron momentum is exaggerated. The vectors are shown radiating from a sphere at the origin on which the angles between vectors appear as arcs of great circles. This sphere is shown merely to aid in visualizing the diagram in three dimensions.

As we are particularly interested in the *breadth* of the shifted line we define a wave-length coordinate, $l = \lambda_2 - \lambda_1 - 2\alpha\lambda_1 \sin^2 \frac{1}{2}\theta$ so chosen that l has its origin at the "center" of the shifted line (shifted position for scattering by free *initially stationary* electrons) and measures the wave-length deviation given by the first term of the right hand member of Eq. (5). Then

$$l = \frac{\lambda_c \cos \theta_1 - \lambda_1 \cos \phi}{1 - \beta_1 \cos \theta_1} \beta_1 \tag{6}$$

in which λ_c is the Compton shifted wave-length for the simple case of an initially stationary electron

$$\lambda_c = \lambda_1 + 2\alpha\lambda_1 \sin^2 \frac{1}{2}\theta.$$

Equation (6) can be much simplified by describing the direction of the initial electron momentum in terms of a new angle Ψ measured from a reference axis⁶ taken in the direction of the change in momentum which the radiation would suffer for the simple Compton case of a stationary electron scattering radiation at the angle θ .

In Fig. 4 let OA be the direction of the incident quantum, OB the direction of the scattered quantum, OC the direction of the electron's initial velocity. Make the vector OA equal in length to λ_c , the vector OB equal in length to

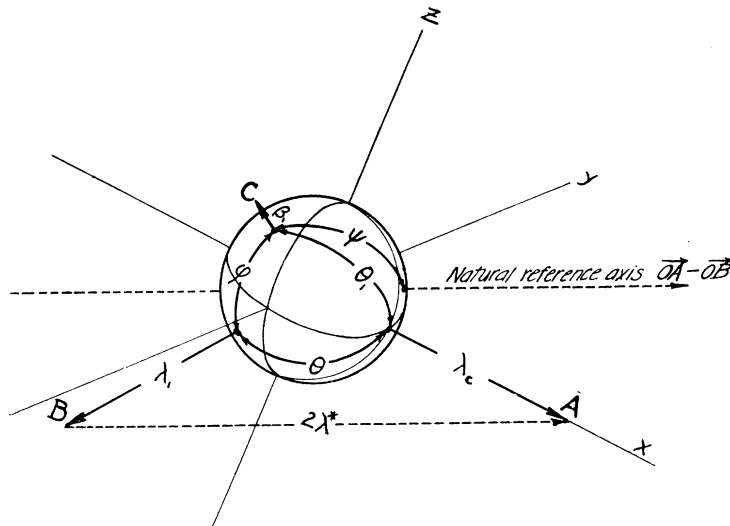


Fig. 4. Illustrating the definition of the "natural" reference axis and of the angle ψ . It should be emphasized that λ_c is the simple Compton shifted wave-length for the case where vector C vanishes ($\beta_1=0$) and that therefore λ_c is constant for a given primary wave-length and scattering angle and the direction of the natural reference axis is a constant. Note that λ_c is taken along the *incident* direction and λ_1 along the *scattered* direction. This inversion is caused by the fact that the momenta are inversely as the wave-lengths.

λ_1 and the vector OC equal in length to β_1 . We define a new wave-length λ^* represented to the same scale by the distance AB . Now note that the numerator of Eq. (6) can be represented in terms of the vectors of Fig. 4 (designated by their termini) as the difference of two scalar products

$$C \cdot A - C \cdot B$$

or what is equivalent $C \cdot (A - B)$

The vector whose length is λ^* is precisely $(\mathbf{A} - \mathbf{B})$ hence if Ψ is the angle between OC and AB we rewrite Eq. (6) as follows

$$l = \frac{\cos \psi}{1 - \beta_1 \cos \theta_1} 2\beta_1 \lambda^* \quad (7)$$

where

$$2\lambda^* = (\lambda_c^2 + \lambda_1^2 - 2\lambda_c \lambda_1 \cos \theta)^{1/2}. \quad (8)$$

The denominator is nearly unity in most practical cases. Thus it is evident that the wave-length deviation l from the simple Compton shift caused by a scattering electron having an initial velocity βc (instead of zero velocity) is proportional to the projection $\beta_1 \cos \Psi$ of the electron's initial velocity along the direction of the vector representing the change in momentum which the radiation would suffer if scattered by an initially stationary electron through the scattering angle θ .⁶

This latter direction is a stationary axis in space independent of the direction of the electrons' initial motion and the projection on it in question can be either positive or negative, i.e. $\cos \Psi$ may have either sign. Thus the extreme values of l are given (if β^2 is considered negligible compared to unity) by the inequality

$$-2\beta_1 \lambda^* + 2\beta_1^2 \lambda^* \cos \frac{1}{2}(\pi - \theta) \leq l \leq 2\beta_1 \lambda^* + 2\beta_1^2 \lambda^* \cos \frac{1}{2}(\pi - \theta) \quad (9)$$

or if the first power of β be considered negligible compared to unity

$$-2\beta_1 \lambda^* \leq l \leq 2\beta_1 \lambda^* \quad (9.1)$$

In either case therefore l can vary over the wave-length range

$$\Delta \lambda = 4\beta_1 \lambda^* \quad (10)$$

for electrons of constant initial speed β_1 and all possible directions of motion.

Case of ensemble of electrons of speed βc and random direction. Since the velocities are uniformly distributed as to direction over the surface of a sphere the probability of scattering by an electron whose velocity makes an angle Ψ to $\Psi + d\Psi$ with the above defined natural reference axis⁷ is

$$P(\psi) d\psi = \frac{1}{2} \sin \psi d\psi. \quad (11)$$

The probability $P(l)$ of a given deviation l from the Compton shift is then to be obtained from Eqs. (7) (11) and the derivative of (7), by eliminating Ψ and $d\Psi$.⁷ This gives

⁶ The vector change in light momentum for scattering at angle θ by an *initially stationary electron* constitutes the natural and appropriate reference axis for the problem of scattering at angle θ by moving electrons.

⁷ This operation is much simplified if the denominator in Eq. (7) be first set equal to unity. This amounts to neglecting β in comparison to unity. θ_1 is a complicated function of the colatitude ψ and the azimuth ϕ . Taking the above defined natural reference axis as polar axis and the plane of the scattering angle as reference plane we have

$$\cos \theta_1 = \cos \psi \cos \frac{1}{2}(\pi - \theta) + \sin \psi \sin \frac{1}{2}(\pi - \theta) \cos \phi$$

$$P(l)dl = (4\beta\lambda^*)^{-1}dl \text{ (approximately)} \tag{12}$$

The relative error committed in this formula is of the order of β . For $\lambda^* = 740$ X.U. $l = 25$ X.U. the error committed is about 3 percent. For narrower parts of the line structure it is even much less. From Eq. (11), since

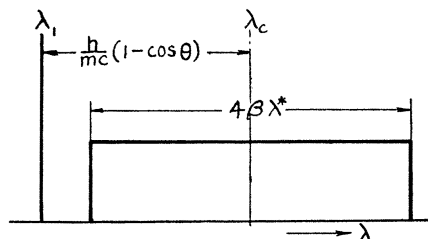


Fig. 5. Spectral distribution curve of originally monochromatic radiation after scattering through angle θ by an ensemble of electrons of initial speeds βc and random directions.

the right hand member is independent of l , it is evident that all deviations l are equally probable within the limits placed by inequality (9). Outside these limits the probability is nihil. Thus (see Fig. 5) a good approximation to the line structure contributed by the randomly directed ensemble of electrons of speeds between β and $\beta + d\beta$ is a rectangular spectral distribution of breadth $4\beta\lambda^*$ and of area proportional to the population of the speed class β to $\beta + d\beta$. (This distribution is not quite centered on the Compton shifted position but as can be seen by reference to inequality (9) is displaced toward longer wavelengths by a slight amount $2\beta\lambda^* \cos \frac{1}{2}(\pi - \theta)$. This shift is wholly inappreciable however for values of β of importance in the experimental case).

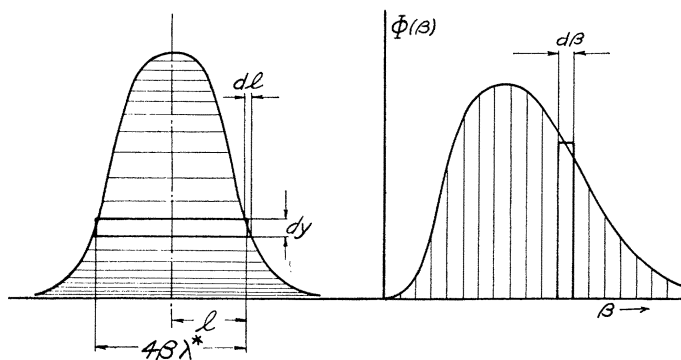


Fig. 6. Illustrating the relation between spectral intensity distribution in the Compton line (left) and population of electron speed states (right). Each elementary rectangle on the left is equal in area to a rectangle on the right while the spectral breadth $4\beta\lambda^*$ of each rectangle on the left is proportional to the abscissa β of the rectangle on the right.

Case of ensemble of electrons with random directions and any speed distribution, $\Phi(\beta)$. The line structure in this case is to be thought of as built up out of an assemblage of rectangles of infinitesimal height each having its

dimensions determined in the same way as the rectangle of Fig. 5. For convenience in adding spectral intensities the rectangles must of course be piled on top of each other in order of decreasing breadth, that is to say decreasing values of β . Referring to Fig. 6 the curve $\Phi(\beta)$ on the right represents the populations of the states or speed ranges β to $\beta+d\beta$ required by the dynamics of the electrons in the solid scattering body while the curve on the left represents the resulting Compton line structure. The elementary rectangular area $2ldy$ in the left hand curve is to be kept proportional to the elementary rectangular area $\Phi(\beta)d\beta$ in the right hand curve. If the constant of proportionality is k we can express the differential equation of the line structure curve in terms of the speed distribution function thus

$$-2ldy = k\Phi(\beta)d\beta \quad (13)$$

since the half breadth of each rectangle is $l=2\beta\lambda^*$ we can replace $d\beta$ by $dl/2\lambda^*$ and β by $l/2\lambda^*$. Dividing Eq. (13) by $-2l$ and integrating from $y=0, l=\infty$ to $y=y, l=l$ we obtain the equation of the line structure curve for continuous functions which vanish as $l \rightarrow \infty$

$$y = -k \int_{l=\infty}^{l=l} l^{-1} \Phi(l/2\lambda^*) dl. \quad (14)$$

Definition of line "breadth." For the purpose of the present investigation we are especially interested in the spectral "breadth" of curves such as shown in Fig. 6 and defined by Eq. (14) and in particular we wish to study the dependence of the breadth on the scattering angle θ . There is no ambiguity

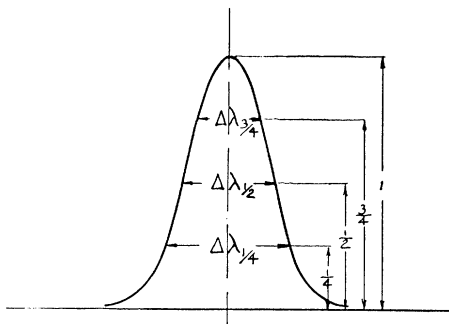


Fig. 7. Illustrating terminology of line breadths.

about the breadth of a rectangular spectral distribution such as is shown in Fig. 5 but real Compton lines resemble more nearly Fig. 6, the scattering electrons being without doubt distributed over a wide range of speeds. We shall speak of the "breadth" $\Delta\lambda_h$ e.g. $\Delta\lambda_{3/4}, \Delta\lambda_{1/2}$ meaning the spectral breadth measured across the line structure at a specified proportion of its height. Thus we mean by $\phi\lambda_{1/2}$ the spectral breadth of the line measured at a point half way up from the background to the peak. See Fig. 7.

Dependence of line breadth on scattering angle. Consider what happens

to the Compton line as the scattering angle is varied, keeping the primary wave-length and the material of the scatterer (and therefore $\Phi(\beta)$) always the same. Under these conditions the only quantity that suffers change is λ^* and referring to Fig. 6 it is evident that all the elementary rectangles of breadth $4\beta\lambda^*$ going to make up the line structure will be horizontally extended or contracted in the same proportion. The breadth just defined above, $\Delta\lambda_h$, will always measure the spectral breadth of the rectangle contributed by one and the same class of electrons of speeds between β and $\beta+d\beta$.

Now λ^* defined in Eq. (8) can most easily be visualized graphically. In Fig. 8 we construct triangles for the values of the scattering angle $\theta = 0^\circ, 22.5^\circ,$

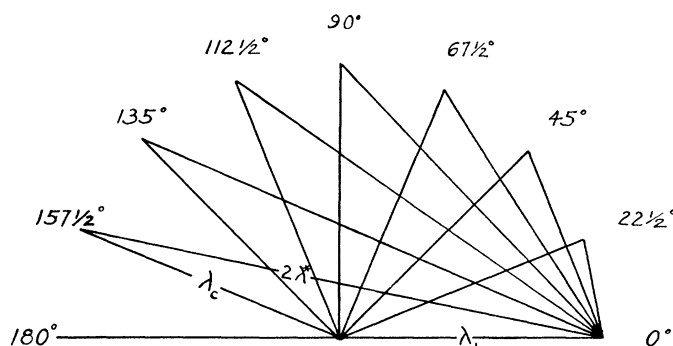


Fig. 8. Graphical construction for λ^* .

$45^\circ, 67.5^\circ, 90^\circ, 112.5^\circ, 135^\circ, 157.5^\circ, 180^\circ$ and make the sides adjacent to θ equal respectively to λ_1 and λ_c where $\lambda_c = \lambda_1 + (h/mc)(1 - \cos \theta)$. The third side of this triangle is $2\lambda^*$. Since λ_c and λ_1 are nearly equal an approximation to λ^* is

$$\lambda^* = \lambda_1 \sin \frac{1}{2}\theta \text{ (approximately)}$$

Hence it follows that the *relative breadth* $\Delta\lambda_r$ as we have already asserted without proof is

$$\Delta\lambda_r = \frac{\Delta\lambda_h}{\Delta\lambda_{h,\max}} = \frac{4\beta\lambda^*}{4\beta\lambda^*_{\max}} = \sin \frac{1}{2}\theta \text{ (approximately).}$$

The reader is referred to Fig. 2 which shows the dependence of relative breadth on scattering angle along with the relative shift. The accurate formula for λ^* , Equation (8), has been used in plotting this curve.

RECAPITULATION OF ASSUMPTIONS

The theory here outlined assumes

1. Conservation of momentum and energy in elementary processes.
2. Electron binding energy negligible compared to energy transferred to electron in scattering process.
3. The initial electron velocity small compared to the velocity of light.

4. Probability of scattering by a given class of electrons proportional to population of the class.

Assumption 1 is in accord with quantum as well as classical mechanics.

Assumptions 2 and 3 are most applicable to precisely those cases of interest for the Compton effect from radiation of about the hardness of MoK radiation. Assumption 4 is probably valid for most of the scattering electrons.⁸

PART II. EXPERIMENTAL

IMPORTANCE OF HOMOGENEITY OF SCATTERING ANGLE

Because the wave-length shift of the Compton modified line depends on the scattering angle the breadth of that line is increased if the scattering angle is not sharply defined in the experimental set up. This spurious breadth due to inhomogeneity of scattering angle was thought by many physicists to be the sole cause of the observed diffuseness of the Compton modified line. At

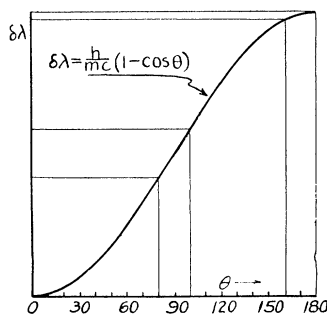


Fig. 9. Illustrating the spurious breadth introduced by a given inhomogeneity of scattering angle at different scattering angles.

only one scattering angle ($\theta = 180^\circ$) a considerable angle inhomogeneity produces very little spurious breadth because the shift has an analytic maximum there. See Fig. 9. Hence several experimenters⁹ have studied the breadth of the modified line at large angles of scattering and concluded that a natural breadth exists. There is some disagreement as to its size however.

For our present purpose it is not possible to resort to the convenient device of working at scattering angles near 180° thereby escaping from the necessity of maintaining a very homogeneous scattering angle. Since we are to examine the dependence of modified line breadth on scattering angle it is necessary to work at a number of angles other than 180° and to maintain these angles very homogeneous in each case. As all who have worked in this field are aware, the requirement of homogeneity of scattering angle is antagonistic to the equally pressing requirement of a large solid angle of radiation

⁸ See Compton's "X-Rays and Electrons," page 291.

⁹ Sharp, Phys. Rev. **26**, 691 (1925); DuMond, Phys. Rev. **33**, 643 (1929), Proc. Nat. Acad. **14**, 875 (1928), Gingrich, Phys. Rev. **36**, 1050 (1930); Nutting, Phys. Rev. **36**, 1267 (1930), Bearden, Phys. Rev. **35**, 1427 (1930).

from the source incident upon the scatterer to give sufficient energy in reasonable exposure times. Unfortunately there are no x-ray lenses to collect x-radiation and render it parallel.

To circumvent these difficulties the authors have constructed the multycrystal spectrograph. This instrument has been described in detail elsewhere¹⁰ and will be touched on but briefly here.

DESCRIPTION OF MULTICRYSTAL SPECTROGRAPH

The instrument consists of fifty small cylindrical units each a Seemann type spectrograph in itself placed vertically on the arc of a horizontal circle of about a half meter radius. Let us call this circle the "major circle" of the instrument. Each unit contains a brass wedge standing at about 0.1 mm

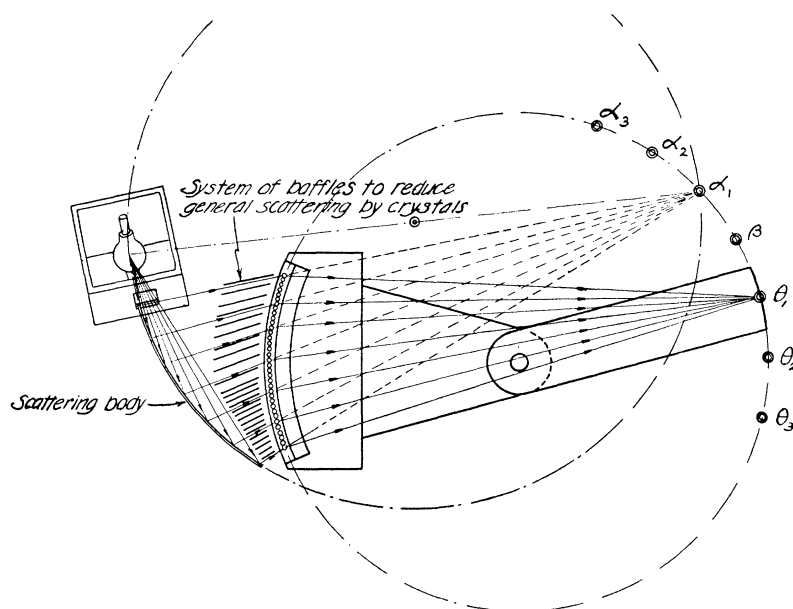


Fig. 10. Geometry of "focussing" and of homogeneity of scattering angle in the multycrystal spectrograph. θ_1 , θ_2 and θ_3 show actual positions of $K\alpha$ line in the first second and third orders respectively. The scattering body is shown set to give homogeneous scattering for the first order.

distance from the cleavage face of a small slip of calcite. The units are orientated so that each calcite will reflect the $K\alpha$ doublet of Mo to exactly the same point on a photographic film coinciding with an arc of the major circle on the opposite side from the bank of crystal units. The geometry of the instrument is such that if one such wave-length coincides or focusses at one point on the circularly curved negative all other wave-lengths and orders will

¹⁰ DuMond and Kirkpatrick. Review of Scient. Insts. **1**, 88 (1930). The principal improvement made in this instrument since the above article was written consists in the addition of fifty individual adjusting levers for the crystals as well as fifty permanently attached mirrors.

also focus at other points on the negative. In Fig. 10 a wave-length λ_1 is shown focussed from all fifty crystals at the point θ_1 . The crystal reflecting planes if produced would all intersect at the point β on the major circle. The incoming radiation, if it were not reflected by the crystals to the point θ_1 , would converge in a point α_1 also on the major circle. α_1 and θ_1 are distant from β on opposite sides by an arc 2θ where θ is the Bragg angle for the wave-length in question. We utilize the fact that the directions of incoming rays are concurrent at α_1 . A second circle is described so as to pass through both the focal spot of the x-ray tube and through α_1 . The scattering body is shaped to coincide with this circle as shown in Fig. 10. Thus the scattering angle is

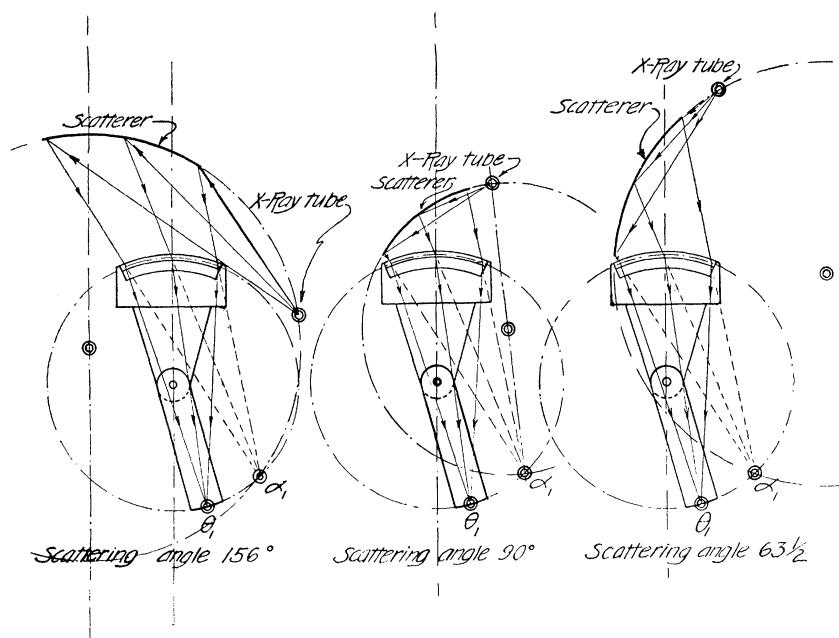


Fig. 11. Geometrical dispositions of x-ray tube, scatterer and spectrograph for the three scattering angles studied.

very nearly homogeneous over all parts of the scatterer. Fig. 11 shows the positions of scatterer, tube and spectrograph for the three angles of scattering which have so far been studied. The principal sources of inhomogeneity of scattering angle are the size of the focal spot of the x-ray tube and the thickness of the scattering body. The use of 50 crystals instead of one permits the tube to be placed much farther away from the scatterer without necessitating unreasonable exposure times and thus permits a great reduction in the inhomogeneity of scattering angle due to the two above mentioned causes.

PRECAUTIONS AS TO PLANENESS OF CRYSTALS AND FOCUSING

At first sight the instrument just described seems fantastically difficult to construct and adjust. As a matter of fact however once a set of fifty good

crystals had been obtained and tested for planeness and a satisfactory orientation method was worked out the task of adjusting them to focus accurately took only about two months. We have been pleasantly surprised to find that the crystals have remained in good adjustment for a period up to the present of about three months.

One of the most exacting and difficult requirements was to get good slips of calcite plane over their entire length. *In studying the Compton effect it is absolutely essential that the crystals be plane over the entire length used in reflecting x-rays.* This is because the scattering body constitutes an *extended source* so that the *entire length* of the crystal reflects x-rays to *each point* on the film. Thus a twisted crystal will give blurred diffused spectral lines with an extended source whereas the same crystal would give sharp but inclined or bent lines with a point source. See Fig. 12. Our first care was therefore to insure that all crystals should be "plane." This we tested by means of primary radia-

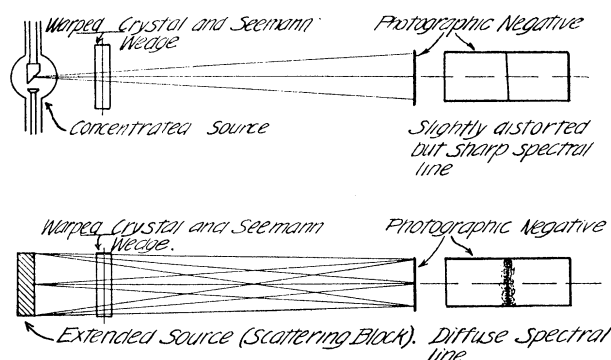


Fig. 12. Illustrating how a warped crystal gives a sharp line with a point source but a blurred line with an extended source.

tion from an x-ray tube placed a short distance from the front of the spectrograph. As the tube was much nearer the crystal than was the negative and had a rather small focal spot only a small portion of the length of the crystal was used in forming the lines on the negative. By moving the x-ray tube up and down parallel to the wedge of the Seemann spectrograph any region in the height of the crystal could be used to reflect spectral lines to the negative. Our practise was to compare in this way the position of lines reflected from four points along the height of the crystal with the lines as reflected from the midpoint of the crystal. Crystals that failed to reflect lines to the same point to within less than half the breadth of a line (or about half an x-unit on our spectrograms) were discarded. The backs of the crystals had to be ground to fit into their holders before such tests had any significance and on account of the numerous discards this constituted one of the most tedious features of the experiment. We take a pardonable pride therefore in calling attention to the great sharpness of the unshifted lines we have obtained. This sharpness bears witness to the planeness and perfection of each and every one of the fifty crystals used as well as to the accuracy with which they are focussed.

The focussing of the crystals was accomplished photographically. After fifty good crystals mounted in the cylindrical Seemann units in the spectrograph had been obtained, one of these near the center was permanently clamped in a predetermined orientation so as to reflect the $\text{MoK}\alpha$ lines in a convenient position on the film. This was called the reference crystal. The other forty-nine units were first roughly orientated by means of a fluorescent screen so as to reflect their lines at the same point on the film to within a few millimeters. Direct radiation was used, the Mo tube being mounted in a lead box in front of the spectrograph on a large wooden sector turning on a pin directly under the point α_1 . Divisions marked on the circular edge of this sector made it possible at a moment's notice to align the tube with any desired crystal. A lead shield was used to isolate all but the crystal under test. The

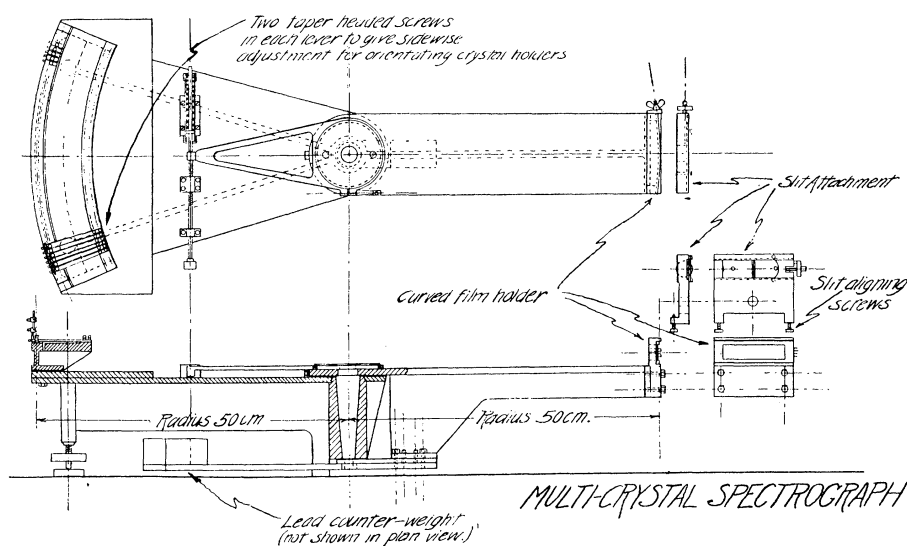


Fig. 13. Plan and elevation of multicrystal spectrograph.

fine adjustment of the crystals by photography consisted in taking a photograph of the $K\alpha$ lines with the reference crystal and then without disturbing the negative taking the $K\alpha$ lines with the crystal to be adjusted. Shields were used in front of the negative so that the reference lines appeared in the middle of the height of the negative while the lines from the crystal under test appeared just above and below. When the focussing of a crystal was acceptable its lines joined those of the reference crystal forming continuous lines across the negative with no perceptible break or jog at the two junction points. Forty-five seconds sufficed to give a good exposure. A complete set of forty-nine such pairs of exposures was made testing the state of adjustment of all crystals against the reference crystal. These exposures appearing on ten pieces of film were all developed, fixed and dried at one time in an especially designed holder, thus economizing enormously on the time over what would be required for separate development. Each crystal was then orientated

through the angle demanded by the error in adjustment indicated in the photographs. This could be done with considerable accuracy, thanks to a small gilded plane mirror permanently mounted on top of each crystal holder. The reflection of a scale 3 meters distant from the mirror was observed with a telescope as a means of measuring the angles through which the crystal must be turned to correct the error indicated on the photographs. After making the indicated orientation adjustments a second set of forty-nine pairs of comparison photographs was taken. A few of the crystals were already found to be in perfectly acceptable focus with respect to the reference lines. These were eliminated from the remainder of the work by dropping small brass covers over their adjusting screws. The cycle was then repeated and each time more and more crystals came into acceptable adjustment until after eleven cycles all had been satisfactorily adjusted.

The fine orientation of the crystals is accomplished by means of a small steel lever, one for each crystal unit, which can be clamped at one end to the projecting shank of the crystal holder. The other end of this lever is given a slight sidewise motion to right or left by two conical headed screws pressing on opposite sides of two conical holes in which they enter loosely. Fig. 13 shows a complete plan and elevation of the entire spectrograph.

PART III. RESULTS

BREADTH NOT DUE TO POOR RESOLUTION OR INSTRUMENTAL DEFECTS

The unshifted lines on the Compton effect exposures play the role of a control on the resolution of the spectrograph. Some workers in this field are under the impression that even the unshifted lines in scattered radiation are broader than the primary lines. Such however is not the case as can be plainly seen on our three spectrograms reproduced in Fig. 14. It is quite evident from an inspection of Fig. 14 that the unshifted lines are very much narrower than the broad diffuse distribution of the Compton modified radiation. It therefore cannot be claimed that the observed breadth of the modified line is caused either by poor resolution, poor focussing of crystals, or any other defect in the spectrograph since this latter quite evidently *gives on the same negative very sharp lines*. The $K\alpha$ doublet in the unshifted position is completely resolved.

No intensifying screens have been used in the exposures with the multi-crystal spectrograph. This eliminates any possible blurring due to poor contact between the intensifying screen and the negative and any falsification of relative intensity that such screens might cause.

X-RAY INTENSITIES AND EXPOSURE TIMES

An ordinary molybdenum target Coolidge water-cooled x-ray tube placed in a lead housing was used as the source of primary radiation. The radiation passed out of the lead housing through a hole of the right size and shape to give a beam which would just illuminate the whole scatterer with about a centimeter to spare all around. The tube was run at from 20 to 25 m.a. and 50 k.v. continuously 24 hours a day. The exposure times were respectively

360 hours, 223 hours and 897 hours for the scattering angles 63° , 90° , and 156° . The long exposures were necessitated by the great distance from the

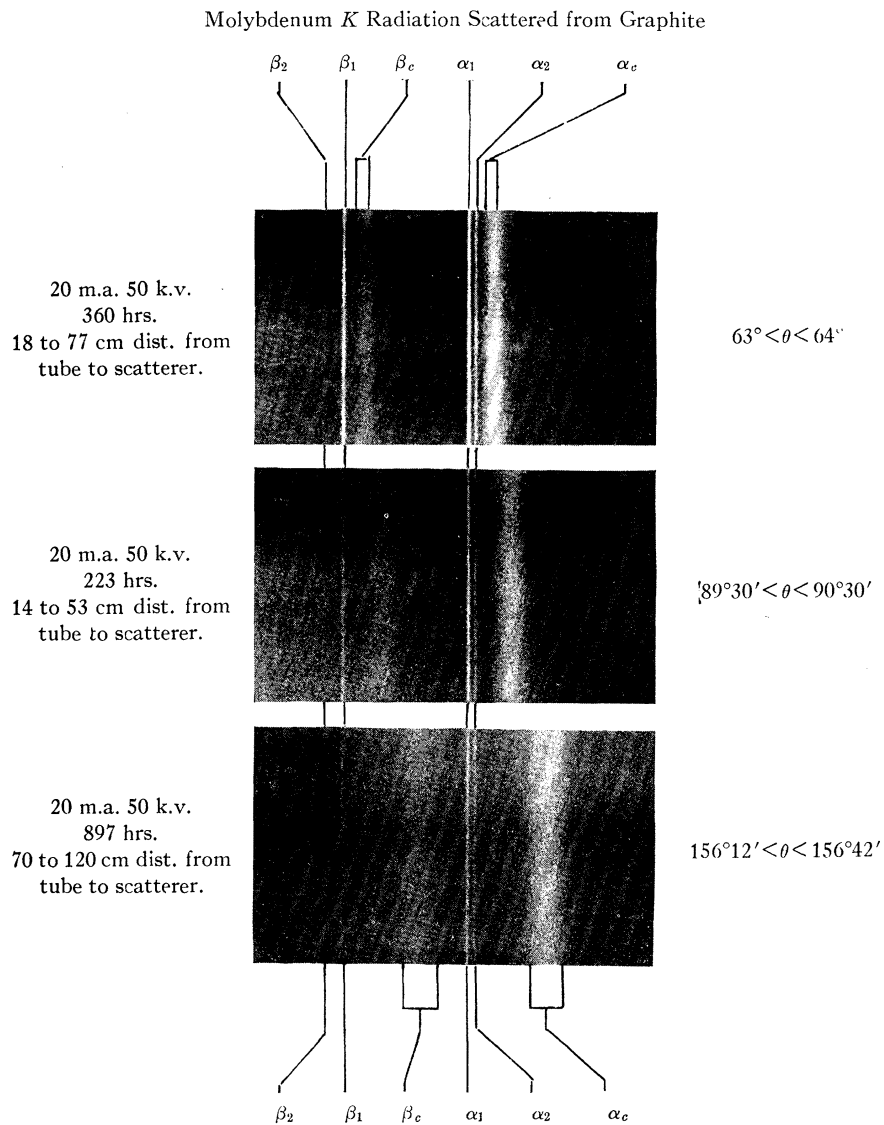


Fig. 14. Spectra of molybdenum *K* radiation scattered at three very homogeneous scattering angles from graphite, taken with the multicrystal spectrograph. Note sharpness of unshifted lines and increasing breadth of shifted lines as the scattering angle increases.

tube to the scatterer. In the case of the 156° exposure the tube was 120 cm from the far end of the scatterer and 70 cm from the near end. The large distance however gives a huge improvement in homogeneity of scattering angle.

HOMOGENEITY OF SCATTERING ANGLE

The greatest inhomogeneity of scattering angle in any case is one degree. The inhomogeneities are indicated in Fig. 14. These inhomogeneities could not possibly produce the observed shifted-line breadth but would on the contrary give a breadth of about the same order of magnitude as the width of the narrower unshifted lines.

To insure this homogeneity of the scattering angle the positions of tube and scatterer were accurately located by means of a radius arm capable of describing the circle on which they and the point α_1 must lie. This radius arm carries a plumb-bob at its outer end which can be lowered into close proximity with the curving scatterer and the point α_1 . The x-ray focal spot is aligned

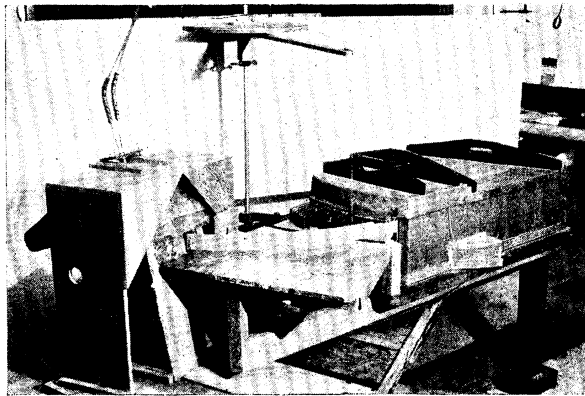


Fig. 15. General view of experimental set-up. Note the radius arm for locating the tube and scatterer, also the baffle plates to reduce background.

with this plumb-bob by sighting from two directions with auxiliary plumb-lines. By measuring the angle through which this radius rod must turn in passing from α_1 to the x-ray focal spot the angle of scattering can be and was measured with more than adequate accuracy. In the general view Fig. 15 of the experimental set-up this radius arm is clearly visible.

MODIFIED LINE BREADTH INCREASES WITH SCATTERING ANGLE

Even a cursory glance at the spectra of Fig. 14 shows that the modified line breadth increases with increasing scattering angle. In order to test this quantitatively we have made microphotometric analyses of these spectra. A few of the microphotometer curves are reproduced in Fig. 16, and in Fig. 17 the theoretical curve of relative breadth is plotted for comparison with the points corresponding to observed breadths. The adjustment to the theoretical curve is made for the grand average of the points corresponding to the *largest scattering angle, the other points falling where they will.* The agreement is seen to be as good as the reproducibility of the breadth measurements.

In measuring the breadth of the shifted β_1 line the effect of β_2 is probably

negligible. In the case of the $\alpha_1\alpha_2$ doublet, however, the shifted radiation due to these two components is confounded in one broad band. It is necessary to decompose this into two similar bands 4 X.U. apart and having the relative intensities 2:1 required by the known ratio of intensities of $\alpha_1:\alpha_2$. This decomposition is done by means of the following device: Referring to Fig. 18

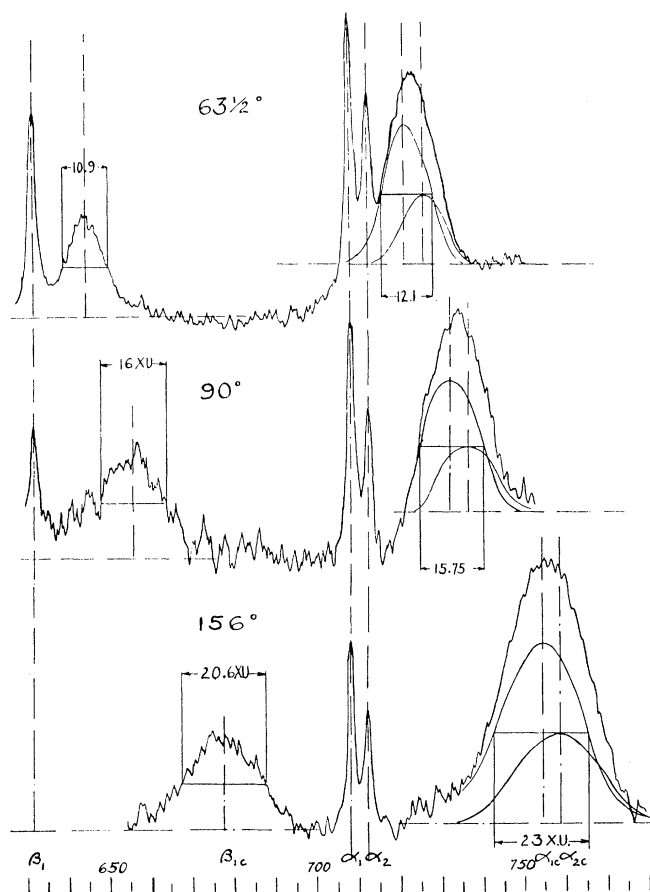


Fig. 16. Microphotometer curves of the spectra shown in Fig. 14. Five such curves (fifteen in all) were obtained for each scattering angle by running the microphotometer slit across the lines in different regions of their height. The three curves here shown are fairly typical of the entire set.

let $F(x)$ be the function representing the observed line structure. Let $f(x)$ be the curve representing the contribution to $F(x)$ made by the α_1 line. Then the contribution made by the α_2 line will evidently be $\frac{1}{2}f(x - \delta)$ where $\delta = 4$ X.U., the known wave-length separation of α_1 and α_2 . We have then that

$$F(x) = f(x) + \frac{1}{2}f(x - \delta)$$

where $F(x)$ is experimentally given and $f(x)$ is to be found. From the experimentally known function $F(x)$ subtract the known function $\frac{1}{2}F(x - \delta)$

$$F(x) - \frac{1}{2}F(x - \delta) = f(x) + \frac{1}{2}f(x - \delta) - \frac{1}{2}f(x - \delta) - \frac{1}{4}f(x - 2\delta).$$

To this in turn add the known function $\frac{1}{4}F(x - 2\delta)$

$$F(x) - \frac{1}{2}F(x - \delta) + \frac{1}{4}F(x - 2\delta) = f(x) - \frac{1}{4}f(x - 2\delta) + \frac{1}{4}f(x - 2\delta) + \frac{1}{8}f(x - 3\delta).$$

Evidently if this process be continued indefinitely we shall have

$$F(x) - \frac{1}{2}F(x - \delta) + \frac{1}{4}F(x - 2\delta) \text{ etc.} = f(x)$$

because the last term neglected will vanish both due to its rapidly decreasing coefficient and due to the diminution in $f(x - n\delta)$ as n becomes large.

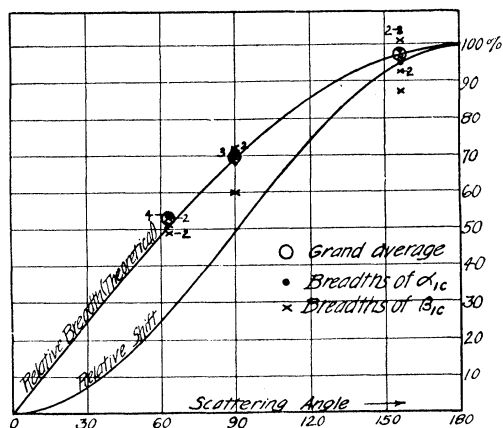


Fig. 17. Measured relative breadths of shifted lines compared with theoretical prediction based on initial electron velocity as the cause of breadth. The full line is the theoretical curve.

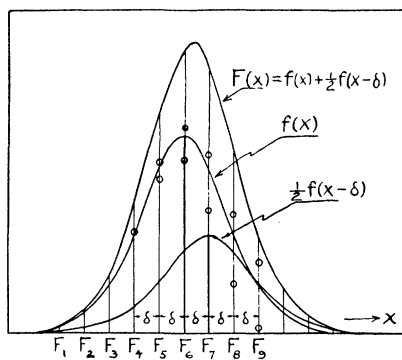


Fig. 18. Illustrating the method of decomposing line structure curves from the $K\alpha$ doublet.

In practise the decomposition can be very rapidly effected graphically by the following procedure. Construct the curve $F(x)$ representing the observed shape of the Compton line to scale and erect equally spaced vertical ordinates

with the spacing δ . The value of the ordinate F_4 say is corrected by subtracting from it half the value of F_3 , its first neighbor to the left, then adding a quarter of F_2 , subtracting an eighth of F_1 , etc., etc., until the amounts to be added to or subtracted from F_4 become negligible. All the ordinates are treated in this same way. By actual trial on curves of the type of the Compton line structure this method has been found to work very well. It is of course an easy matter to check the work by adding the two components obtained in the decomposition process and comparing the sum with the original curve.

In Table I the observed breadths of α_{12c} and β_{1c} at half maximum height are recorded for the three scattering angles studied. Measurements on five microphotometer curves taken across the spectral lines in different regions of their height are recorded for each scattering angle. The tabulated breadths of α_{1c} were obtained graphically by the decomposition method described above.

TABLE I. Breadths in x -units $\Delta\lambda_3$.

$63\frac{1}{2}^\circ$			90°			156°			Micro- photo- meter Run
α_{12c}	α_{1c}	β_{1c}	α_{12c}	α_{1c}	β_{1c}	α_{12c}	α_{1c}	β_{1c}	
13.0	12.1	12.0	16.2	15.6	13.3	22.4	22.8	22.4	1
12.4	11.5	10.9	16.4	15.75	16.0	21.8	21.2	19.4	2
13.0	12.1	11.5	15.75	15.15	15.75	23.0	23.0	20.6	3
13.0	12.1	12.1	16.4	15.75	16.0	23.0	23.0	20.6	4
13.0	12.1	10.9	16.4	15.75	15.2	22.2	21.9	21.5	5
12.9	12.0	11.5	16.2	15.6	15.2	22.5	22.4	20.9	Average
11.8			15.4			21.6			Grand average of α_{1c} and β_{1c}
51%			69%			97%			Theoretical relative Breadths

MODIFIED LINE BREADTH INCREASES WITH PRIMARY WAVE-LENGTH

Attention is called to the fact that in Table I the average breadths of α_{1c} are systematically higher than the average breadths of β_{1c} . We do not feel that the precision of our breadth measurements justifies more than a claim to a qualitative agreement with theory in this respect. It is interesting to note however that in each case the longer primary wave-length gives the broader shifted line and that the breadths are in about the same proportion as the wave-length in agreement with the formulae

$$\Delta\lambda = 4\beta\lambda^*$$

$$\lambda^* = (\lambda_1^2 + \lambda_c^2 - 2\lambda_1\lambda_c \cos \theta)^{1/2}$$

$$\lambda_c = \lambda_1 + \frac{h}{mc}(1 - \cos \theta)$$

CAUSE AND ELIMINATION OF HEAVY BACKGROUND

It has been noted by many observers that the background intensity relative to the line intensity in the spectra of scattered radiation is much stronger

than in the case of the primary radiation. Many explanations have been offered for this, all of which probably contributed to the effect in some small measure. We believe that we now have unquestionable evidence however that the great bulk of this enhanced background effect is due to non-selective scattering at the crystals and crystal wedges. General, amorphous, or non-selective x-ray scattering by the crystal in a spectrograph is due to scattering of the modified Compton type. Such scattering is incoherent and hence non-selective as to wave-lengths. It is also non-specular, i.e. the conditions of equality of incidence and reflection angles is not imposed. This means that a given point on the negative can receive radiation of all wave-lengths by this scattering process from all parts of the scattering body. This same point on the negative can by spectrally selective Bragg reflection only receive one wave-length scattered from one very small portion of the scattering body. Hence, though the modified scattering may be small, it is greatly favored by the fact that it is integrated over a wide range of continuous spectrum and over a broad solid angle as large as the scatterer can subtend. With these considerations in mind we have tried the effect of introducing a set of baffle plates in front of the spectrograph in such a way as to greatly limit the solid angle of radiation which can be collected at the crystal and wedge. With these baffles in place each crystal can only "see" a very small segment of the scatterer about three centimeters long at most whereas without the baffles each crystal was exposed to scattered radiation from a large part of the entire 55 cm length of the scatterer. The baffles leave plenty of room for the formation of the entire shifted and unshifted K spectrum however which only covers a range of about three degrees. These baffles can plainly be seen in the general view Fig. 15. See also Fig. 10.

The result of introducing the baffles was most striking. Whereas without the baffles the back-ground fogging of our negatives was so strong as to nearly obscure the unshifted and shifted lines, rendering the negatives quite hopeless for reproduction *this background was entirely suppressed as soon as the baffles were introduced*. We feel certain therefore that the non-specular, non-selective scattering at the crystal faces and wedges is responsible for the heavy background.

MEASUREMENTS OF SHIFT

As a check on the Compton formula for the shift, $\delta\lambda = (h/mc)(1 - \cos \theta)$ we have plotted in Fig. 16 the positions predicted for the shifted lines by the above formula assuming $h/mc = 24.2$ X.U. as computed from present accepted values of these constants. The agreement is good and seems to eliminate the possibility of a 9 percent deviation from this value reported recently by other observers.¹¹

CRITICAL DISCUSSION OF RESULTS

The line breadths which we have observed and reported in this paper are not in accord with the observations of two other observers, namely J. A.

¹¹ Davis and Mitchell, Phys. Rev. **32**, 331 (1928).

Bearden¹² and N. S. Gingrich¹³ both of whom have studied the breadth of the modified line at large scattering angles (to reduce the broadening from angular inhomogeneity) using the double crystal spectrometer. These experimenters obtain lines broader than the unshifted lines but still sufficiently narrow to show partial resolution in the case of the shifted $K\alpha$ doublet. P. A. Ross, using his ingenious balanced filter method, also seems to observe a partial resolution of this doublet. This method however does not give very distinct evidence as to the breadth of the shifted line. Ross' and Bearden's primary wave-lengths were somewhat shorter than those used in the present investigation and Ross' angles of scattering are smaller. Both these conditions would, if the theory presented in this paper is correct, tend to give these observers a somewhat narrower shifted line¹⁴ than that here reported. N. S. Gingrich however reports narrower lines than ours under conditions nearly identical to ours. Indeed his scattering angle is larger and is inhomogeneity of scattering angle about twenty times as great as ours. His modified $MoK\alpha$ radiation observed with the double crystal spectrometer appears as two sharply pointed peaks partially resolved at the base. We are completely at a loss to explain the discrepancy between our results and his. Examination of our photographic spectrograms (here reproduced Fig. 14) shows not the slightest suggestion of resolution of the shifted $K\alpha$ doublet although the resolution of our spectrometer as proved by our well resolved unshifted lines is amply sufficient for this purpose. The principal difference between Gingrich's conditions and ours was the use of the double crystal (high resolution) spectrometer in place of our multicrystal spectrometer, the use of much greater x-ray intensities incident on his scatterer than ours and the presence of much greater inhomogeneity of scattering angle in his case than in ours.

On the other hand however recent photographic results published by F. L. Nutting¹⁵ show a *broad* modified β_1 line in good agreement with our modified line breadths and much too broad to permit of resolution of two lines as close as $MoK\alpha_{1,2}$. Our present modified line breadths are also in good qualitative agreement with those obtained previously by DuMond¹⁶ for aluminum and beryllium scatterers with a photographic method at large scattering angles. (As the scatterers are different no more than qualitative agreement is to be looked for here). Finally our line breadths agree with those obtained photographically by Sharp¹⁷ under large and homogeneous scattering angles and with primary radiation and scattering substance substantially the same as ours.

We cannot understand why the photographic methods *used with adequate resolution* should yield broader modified lines than the double crystal spectrometer. Perhaps some hitherto unsuspected parameter affects modified line

¹² J. A. Bearden, Phys. Rev. **35**, 1427 (1930).

¹³ N. S. Gingrich, Phys. Rev. **36**, 1050 (1930).

¹⁴ J. W. DuMond, Phys. Rev. **36**, 146 (1930).

¹⁵ F. L. Nutting, Phys. Rev. **36**, 1267 (1930).

¹⁶ DuMond, Phys. Rev. **33**, 643 (1929); DuMond, Proc. Natl. Acad. **14**, 875 (1928).

¹⁷ Sharp, Phys. Rev. **26**, 691 (1925).

breadth. Such parameters might be the x-ray intensity incident on the scatterer or the electrical potential of the scatterer. These seem highly unlikely.

We are now carefully investigating the possibility that multiple scattering may exaggerate our line breadths. Our method of doing this is to make an exposure at 156° with a scatterer cut up into small pieces with intervening properly orientated lead baffles which will almost entirely eliminate the possibility of multiple scattering. There are two reasons why we can almost certainly predict a negative result from this control experiment.

First, the scattered radiation from the entire scatterer at a point outside the direct beam but not far distant from the scatterer itself can be faintly seen on a fluorescent screen. At this point it is certainly less than one percent of the intensity of direct radiation incident on the scatterer. It seems then unlikely that the ratio of intensity of scattered radiation from the scatterer incident a second time on the scatterer to primary intensity should be more than one percent and this is too small to account for the discrepancy between our modified line breadth and that of Gingrich.

Second, our present modified line breadths are in agreement with those above mentioned of Sharp, Nutting and DuMond, each of which was obtained under conditions which should give if anything less double and multiple scattering than Gingrich had.

Absolute breadths of shifted lines. Our purpose in this article has been especially to test the *functional dependence* of the natural breadth of the shifted lines on scattering angle and primary wave-length and to compare this with the functional dependence to be expected if the initial velocities of the scattering electrons cause the breadth. We hope to present in the near future a careful study of the electron velocity distributions to be expected from the shapes of our line structure curves. We will state at the present time merely that the breadths of our lines do not seem inconsistent with the velocities to be expected in the carbon atom. A very considerable task of theoretical computation and reduction of our experimentally observed curves remains to be performed before we can definitely draw a favorable or unfavorable comparison between observation and theory on this point. Our observed breadths at half maximum recorded in this paper correspond to a class of electrons the ratio of whose velocities to the velocity of light is $\beta = 0.0076$. This is equivalent to about 15 volts.

In conclusion we wish to express our appreciation of Dr. Millikan's support of this research and of the patience and skill of Julius Pearson, our instrument maker, who developed the technique and did the tedious work of grinding and fitting the small calcite units into their holders.

NOTE ADDED TO PROOF: We have just developed a 900-hour exposure at 156° scattering angle with a graphite scatterer divided into fifty parts by lead baffles so orientated as to permit the entrance of the incident radiation and the exit of the scattered radiation, but arranged to prevent any multiple scattering by exchange of radiation from one unit to another. The units have smaller dimensions than the scatterer used by N. S. Gingrich. We believe therefore that our multiple scattering should be less than his. *The Compton line however on this exposure appears with the same breadth as the one reproduced in this paper.*

Molybdenum *K* Radiation Scattered from Graphite

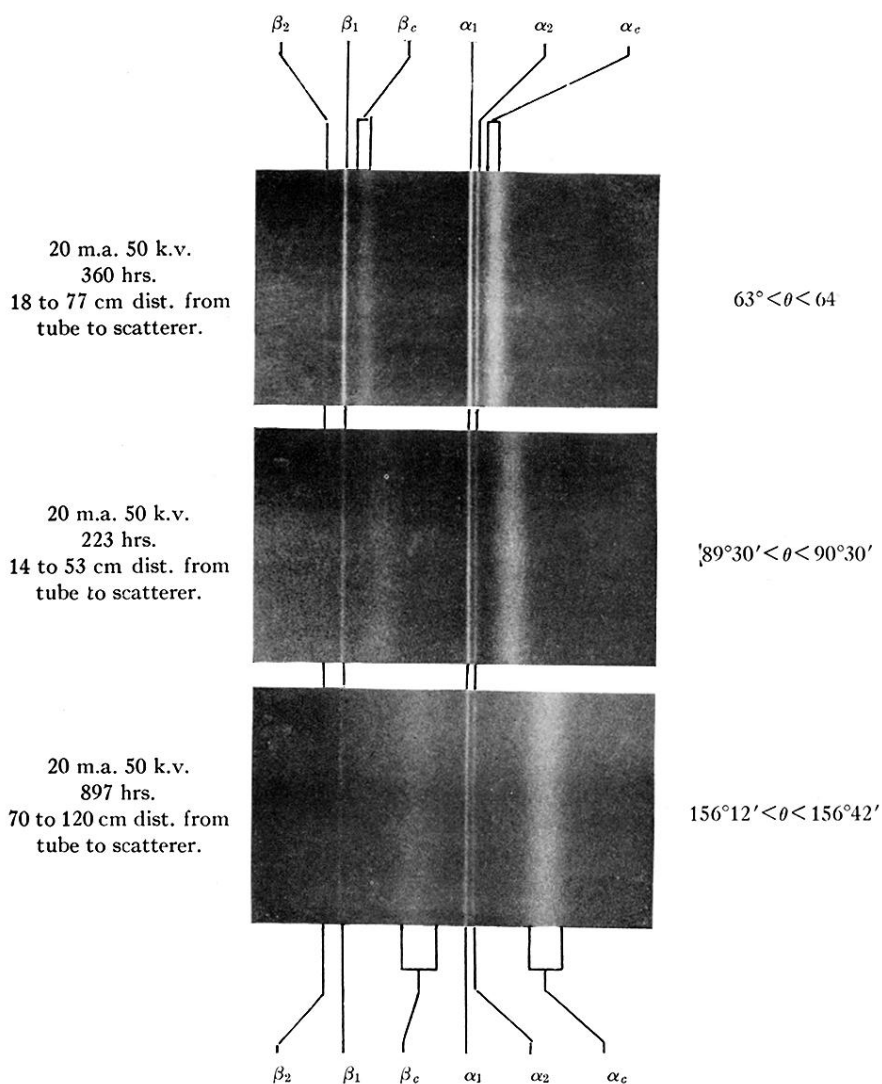


Fig. 14. Spectra of molybdenum *K* radiation scattered at three very homogeneous scattering angles from graphite, taken with the multicrystal spectrograph. Note sharpness of unshifted lines and increasing breadth of shifted lines as the scattering angle increases.

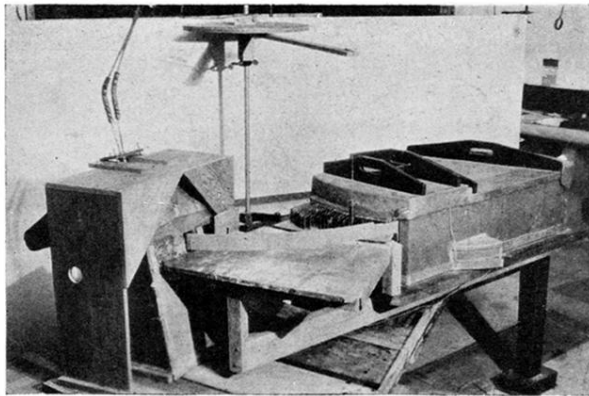


Fig. 15. General view of experimental set-up. Note the radius arm for locating the tube and scatterer, also the baffle plates to reduce background.